Pathological oligodendrocyte precursor cells revealed in human schizophrenic brains and trigger schizophrenia-like behaviors and synaptic defects in genetic animal model

Jian-Qin Niu (jianqinniu@tmmu.edu.cn)
Third Military Medical University

Guangdan Yu
Third Military Medical University

Yixun Su
Third Military Medical University

Chen Guo
Zhejiang University school of Medicine

Chenju Yi
National University of Singapore

Bin Yu
Third Military Medical University

Hui Chen
University of Technology Sydney https://orcid.org/0000-0001-6883-3752

Yihui Cui
Zhejiang University School of Medicine

Xiaorui Wang
Third Military Medical University

Yuxin Wang
Third Military Medical University

Xiaoying Chen
Third Military Medical University

Shouyu Wang
Third Military Medical University

Qi Wang
Third Military Medical University

Xianjun Chen
Chongqing Medical University

Xuelian Hu
Third Military Medical University

Feng Mei
University of California, San Francisco
Alexej Verkhratsky
The University of Manchester
Lan Xiao
Third Military Medical University

Article

Keywords: Myelin, Synapse, DISC1, Wnt/β-catenin pathway, GSK3β, Wif1

Posted Date: March 31st, 2022

DOI: https://doi.org/10.21203/rs.3.rs-1496764/v1

Abstract

Although the link of white matter to pathophysiology of schizophrenia is documented, loss of myelin is not detected in patients at the early stages of the disease, suggesting that pathological evolution of schizophrenia may occur before significant myelin loss. Disrupted-in-schizophrenia-1 (DISC1) protein is highly expressed in oligodendrocyte precursor cells (OPCs) and regulates their maturation. Recently, DISC1-Δ3, a major DISC1 variant that lacks exon 3, has been identified in schizophrenia patients, although its pathological significance remains unknown. In this study, we detected in schizophrenia patients a previously unidentified pathological phenotype of OPCs exhibiting excessive branching. We replicated this phenotype by generating a mouse strain expressing DISC1-Δ3 gene in OPCs. We further demonstrated that pathological OPCs, rather than myelin defects, drive the onset of schizophrenic phenotype by hyperactivating OPCs' Wnt/β-catenin pathway, which consequently upregulates Wnt Inhibitory Factor 1 (Wif1) leading to the aberrant synaptic formation and neuronal activity. Suppressing Wif1 in OPCs rescues synaptic loss and behavioral disorders in DISC1-Δ3 mice. Our findings reveal the pathogenetic role of OPC-specific DISC1-Δ3 variant in the onset of schizophrenia and highlight the therapeutic potential of Wif1 as an alternative target for the treatment of this disease.

Introduction

Schizophrenia, a complex and severe psychiatric condition[1], is one of the 15 leading causes of disability, affecting 1 in 300 people worldwide[2,3]. Although highly heritable, the pathophysiological mechanisms of schizophrenia have not been well understood. Clinical evidence has linked white matter abnormalities to schizophrenia symptoms[4]. Pathophysiological changes include impaired oligodendrocyte differentiation, myelination, and white matter loss[5-7]. However, several diffusion tensor imaging (DTI) studies found no changes in the white matter volume during the early stages of schizophrenia[8-11], suggesting that early pathogenesis of schizophrenia may precede significant myelin loss.

DISC1, as one of the schizophrenia risk genes, regulates OPC maturation and subsequent myelination[12,13]. The RNA-sequencing analyses in both humans and mice demonstrated that OPCs express higher levels of DISC1 when compared to neurons or mature oligodendrocytes (OLs)[14,15], raising a possibility that the high presence of DISC1 in the OPCs may contribute to the pathogenesis of schizophrenia. It was also reported that DISC1 affects hippocampal structure and function, increasing the risk of schizophrenia[16]. Indeed, several DISC1 splicing variants are upregulated in the hippocampi of schizophrenia patients[17-19], where significant pathological changes occur at the clinical high risk (CHR) stage of the onset of schizophrenia[20]. Among these variants, DISC1-Δ3, a splicing variant that lacks exon 3, is one of the most upregulated in multiple brain regions[18,19], although little is known of its role in oligodendroglia in the pathogenesis of schizophrenia.

In the present study, we revealed previously unknown pathological hypertrophied OPCs in schizophrenia patients. We were able to replicate these pathological OPCs in a newly generated transgenic mouse

strain, which mimics the heterozygous DISC1 exon 3 splicing by removing the DISC1 exon 3 from a single allele in oligodendroglial lineage cells. Mechanistically, we demonstrated that mice with enhanced DISC1-Δ3 variant expressed in OPCs demonstrate schizophrenia-like behaviors and synaptic defects, both driven by the overactivated Wnt/β-catenin-Wnt inhibitory factor 1 (Wif1) cascade. Our results provide an alternative insight into the critical role of malfunctional OPCs in pathogenesis of schizophrenia and highlight a molecular target, Wif1, for developing potential therapeutic strategies.

Results

OPCs are hypertrophic in schizophrenia patients

We examined the histological properties of the OPCs in postmortem brain tissues of schizophrenia patients and age-matched healthy controls (Figure S1A). The Sholl analysis of NG2-positive OPCs revealed previously unidentified hypertrophic morphotype in the hippocampus, prefrontal cortex and amygdala of schizophrenia patients when compared to the age-matched healthy controls in both human paraffin tissue sections (Figure 1A-I) and frozen sections (Figure S1B-G). The OPCs in post-mortem tissues of schizophrenia patients displayed a significant increase in the mean number of branches (increased by 73.4 ± 6.9%, 35.3 ± 4.0% and 21.8 ± 3.9% respectively in the hippocampus, prefrontal cortex and amygdala in paraffin human brain tissue sections, Figure 1A-I; increased by 42.1 ± 12.5% and 40.6 ± 14.3% respectively in the hippocampus and prefrontal cortex in frozen sections, Figure S1B-G) and greater mean branch length (increased by 64.7 ± 7.6%, 31.3 ± 3.1% and 24.9 ± 5.3% in paraffin tissue sections, Figure 1A-I; increased by 42.9 ± 9.7% and 57.8 ± 13.8% in frozen sections, Figure S1B-G). In contrast, neither the number of NG2-positive OPCs (paraffin section, Figure 1B, E, H; frozen section, Figure S1C, F) nor the number of OLIG2-positive oligodendroglial cells (paraffin section, Figure 1J-M) per area unit was affected in schizophrenia patients. This is the first time demonstration of hypertrophic pathological OPCs in schizophrenia patients.

Enhanced DISC1-Δ3 expression in the oligodendroglia replicates the hypertrophic OPC in patients

DISC1 is a schizophrenia risk gene and regulates oligodendroglial development[12,13]. The gene sequence of DISC1 is highly conserved between humans and mice (Figure S2A). Re-analyzing RNA-sequencing libraries[14,15] showed that DISC1 expression in human and mouse OPCs is much higher than in newly-differentiated oligodendrocytes, mature oligodendrocytes, and neurons (Figure S2B, C). Analysis of mRNA expression of DISC1 splicing variants revealed that Δ3 and Δ7/8 (DISC1 alleles lacking exons 3, 7 or 8) were downregulated during early brain development (Figure S2D), but upregulated in schizophrenia brains[18].

To mimic pathological changes in schizophrenia patients, we generated a DISC1 $^{exon3\ flox}$ mouse strain, and crossed it with the OPC-specific NG2^{CreERT} mice to obtain NG2^{CreERT}:DISC1$^{exon3\ fl/+}$ (DISC1-Δ3) mice

(Figure 2A). Tamoxifen administration removed a single copy of the DISC1 exon 3 from one allele on the double helix, which replicates enhanced expression of DISC1 exon 3 splicing in schizophrenia patients without affecting the expression of full-length DISC1 gene[18,21] (Figure S2E-G). The efficiency of genetic modification was confirmed by increased mRNA and protein levels of DISC1-Δ3 in the brain; at the same time expression of full-length DISC1 or DISC1 Δ7/8 remained unchanged (Figure S2E-F). The cell-specific expression of DISC1-Δ3 was confirmed by significantly upregulated mRNA levels selectively in OPCs, but not in other brain cell types (Figure S2G).

Consistent with abnormal myelination detected in familiar schizophrenia due to disrupted DISC1 expression[13], the overexpression of DISC1-Δ3 variant in oligodendroglia didn't affect the total number of oligodendroglial lineage cells (Figure 2B), but impaired oligodendrocyte differentiation (Figure 2D-E), decreased the number of myelinated axons (Figure 2F-G) and reduced the myelin thickness (Figure 2F-G). Increased expression of DISC1-Δ3 variant in the newly generated transgenic mouse strain replicated the OPC hypertrophy in schizophrenia patients, as shown by the enlarged PDGFRa (increased by 91.6±16.5% (Figure 2H-I) and $NG2^{CreERT}$:tdTomato labeling areas per cell (increased by 32.4±8.5%) (Figure 2J-K). In contrast, oligodendroglial proliferation was not altered in DISC1-Δ3 mice, as shown by the Ki67/Olig2 quantification (Figure S3A). The morphological appearances of astrocyte, microglia, and the vasculature were not affected by increased DISC1-Δ3 variant expression in oligodendroglia (Figure S3B-E).

Taken together, our results reveal hypertrophic morphology of OPCs in both schizophrenia patients and DISC1-Δ3 mice. The hypertrophic OPCs may be considered as a disease hallmark.

Oligodendroglial DISC1-Δ3 variant triggers schizophrenia-like behaviors and synaptic defects

At postnatal day (P)25 to P36, the age of mice approximately corresponding to human adolescence (12-18 years old) when the first episode of schizophrenia usually occurs[1,22], enhanced oligodendroglial DISC1-Δ3 splicing resulted in schizophrenia-like sensorimotor gating impairment as reflected by the prepulse inhibition test (Figure 3A), as well as by the positive symptoms[23] in the open field test and cliff avoidance test (Figure 3B-C). However, no negative symptoms (assessed by the social interaction test, Figure 3D), motor deficit (travel distance in the open field test, Figure 3B), or memory impairments (novel object recognition test, Figure 3E) were detected in DISC1-Δ3 mice.

Excitation-inhibition disbalance contributes to the pathophysiology of schizophrenia[24,25]. We found that expression of DISC1-Δ3 in oligodendroglia suppressed synaptogenesis, as indicated by the decreased levels of $SYN1^+$ presynaptic and $HOMER1^+$ postsynaptic markers in hippocampal and cortical regions at P25 (Figure 3F, G). Specifically, the number of excitatory synapses labeled with vGLUT1 antibodies but not the inhibitory synapses labeled by vGAT antibodies was reduced in the hippocampal CA1 region (Figure 3F, H). These changes recapitulate decreased excitatory/inhibitory synapses ratio observed in schizophrenia patients[24,25]. In agreement with synaptic alteration, expression of DISC1-Δ3 in cells of

oligodendroglial lineage reduced the frequency of spontaneous excitatory postsynaptic currents (sEPSC) and increased the frequency of spontaneous inhibitory postsynaptic currents (sIPSC) (Figure 3I-K).

To conclude, deletion of DISC1 exon 3 in oligodendroglia is sufficient to induce schizophrenia-like behavioral abnormalities and cause significant synaptic alterations.

Aberrant OPC but not defective myelin contributes to the onset of schizophrenia-like symptoms in DISC1-Δ3 mice

Oligodendroglial DISC1-Δ3 affects both OPC and myelin as presented above. To distinguish the contribution of hypertrophic OPCs from the myelin deficiency during the onset of schizophrenia, we investigated conditional DISC1 exon 3 deletion at different ages. First, we induced oligodendroglial DISC1 exon 3 deletion at P4 - P7 and analyzed the neurological outcome at P10, before the occurrence of myelin defects in the hippocampus (Figure 4A-C, S4A-B). Second, we triggered DISC1 exon 3 deletion between P4 - P7, but analyzed the histological and behavioral changes at P50, when the mature OL numbers, myelin densities and structures in DISC1-Δ3 mice attained a level similar to the wildtype littermates (Figure 4A-E, S4A-C). However, since we cannot rule out the possibility that myelin defects in other brain regions may affect hippocampal synaptogenesis, whereas myelin defects in early life (e.g., the neonatal period in this study) may exert prolonged effects on synaptic development in later life (e.g., puberty in this study), we induced the DISC1-Δ3 deletion at a later stage (between P40 - P45), when the majority of myelin sheaths are established. We assessed the histological and behavioral changes at P50, when no OPC differentiation or myelin deficit was found (Figure 4A-E, S4A-C). In all three experiments, the $NG2^+$ areas per cell in DISC1-Δ3 mice at the endpoints increased by 110.1 ± 20.5%, 280.9 ± 65.0%, and 259.2 ± 60.4% respectively (Figure 4G-I, S4D-E). These OPCs were in close contact with the cell bodies of $NeuN^+$ neurons with synaptic defects (Figure 4J-N). However, the number of $Olig2^+$ cells remained unchanged in all three experiments (Figure S4F).

The absence of myelin deficiency allowed us to investigate the contribution of DISC1-Δ3 OPCs to the above mentioned synaptic defects and schizophrenia-like behaviors. We found that pre- and post-synaptic compartments were significantly reduced in the hippocampus in all three experimental groups (Figure 5A, S5). Golgi staining confirmed decreased number of dendritic spines in DISC1-Δ3 mice at P10 (Figure 5B). Moreover, enhanced DISC1-Δ3 splicing in OPCs was accompanied with decreased sEPSC frequency as early as at P10, whereas deletion at both early and later ages caused behavioral changes at P50 (Figure 5C-F). These results indicate that interfering with OPC DISC1-Δ3 expression alone is sufficient to induce synaptic dysfunction and schizophrenia-like behaviors.

In order to further confirm that aberrant OPCs but not mature OLs contribute to the neuronal defects during the onset of schizophrenia, we cross-breed the $DISC1^{exon3\ flox}$ mice with the OL-specific PLP^{CreERT} mice to obtain PLP^{CreERT}:$DISC1^{exon3\ fl/+}$ mice (OL DISC1-Δ3, Figure 5G). Tamoxifen administration

specifically removed a single copy of the DISC1 exon 3 from one allele in OLs (DISC1-Δ3 OLs, Figure 5G). In the hippocampus of these mice at P21, enhanced expression of DISC1-Δ3 in OLs didn't change the numbers of $SYN1^+$ synaptic puncta (Figure 5H). In addition, neither the morphology of $PDGFR\alpha^+$ OPCs, MBP^+ myelin structures, nor numbers of $CC1^+$ mature OLs and $Olig2^+$ oligodendroglial lineage cells (Figure 5I-J; S4G-H) were affected. These results suggest an OPC-specific manner to initiate schizophrenia-like pathological changes in the DISC1-Δ3 mice.

Subsequently, we performed *in vitro* experiments to confirm the direct impact of DISC1-Δ3 OPCs on neurons. Primary OPCs were isolated from the brains of DISC1-Δ3 and non-CreERT wild-type mice at P7 by immunopanning. They were either co-cultured with hippocampal neurons, or used for medium conditioning to treat the hippocampal neurons. Cultured DISC1-Δ3 OPCs showed hypertrophic morphology similar to that observed in DISC1-Δ3 mice (Figure 5K). Neuronal synapse formation in cells co-cultured with DISC1-Δ3 OPC or exposed to DISC1-Δ3 OPC generated conditioned medium was significantly suppressed (the number of synapses decreased by 58.0 ± 13.3% and 23.5 ± 5.2% respectively, Figure 5L-M).

Collectively, our results demonstrate that pathological OPCs and not myelin defects are the main contributors to the onset of schizophrenia-like symptoms. In addition, DISC1-Δ3 OPCs affect neuronal synaptic formation in a paracrine manner.

Hyperactivity of Wnt/β-catenin pathway in OPCs from schizophrenia patients and DISC1-Δ3 mice

To gain an insight into underlying molecular mechanisms, RNA-sequencing was performed in the OPCs from DISC1-Δ3 and non-CreERT wildtype mice (Figure S6A-C). The Kyoto Encyclopedia of Genes and Genomes (KEGG) analysis indicated significantly increased activity of Wnt/β-catenin pathway in DISC1-Δ3 OPCs (Figure 6A). This was deduced from a 56.9 ± 14.0% reduction in phosphorylated β-catenin (the degraded form of Wnt signaling stimulator), 44.8 ± 15.0% reduction in autophosphorylation of glycogen synthase kinase 3 b (GSK3β) at Tyrosine 216 (Y216, the functional form of an inhibitor of the Wnt/β-catenin pathway), and a 76.3 ± 20.3% increase in the phosphorylated GSK3β at Serine 9 (S9, Figure 6B, S6D) that inactivates GSK3β[26-28]. In addition, a significant upregulation of Wnt downstream targets Axin2 and Notum was detected (199.3 ± 25.7% and 412.2 ± 133.7% increase, respectively, Figure 6C), which also indicates an overactivated Wnt/β-catenin pathway in DISC1-Δ3 OPCs.

Subsequently, we investigated how DISC1-Δ3 deletion affects Wnt/β-catenin signaling in the OPCs. DISC1 is known to directly interact with GSK3β and suppress its Y216 autophosphorylation [28,29]. Thus, DISC1 can inhibit GSK3β function and consequently activate Wnt/β-catenin pathway[29]. Furthermore, DISC1 can also bind to the C-terminal (amino acids 347–854) of Girdin to prevent activation of AKT[30], a suppressor of GSK3β by phosphorylating its S9 residue[30,31], resulting in the indirect regulation of Wnt/

β-catenin pathway. Co-immunoprecipitation analysis showed that DISC1-Δ3, which contains one of the GSK3β binding sites (amino acids 1-220), was still able to directly interact with GSK3β to suppress GSK3β Y216 autophosphorylation (Figure 6D, S6D). However, DISC1-Δ3 structurally lacks the binding site for Girdin and thus cannot bind to it (Figure 6D, S6D), which enables Girdin to activate AKT signaling[30]. Consistently, an increased activity of AKT in DISC1-Δ3 OPCs was also observed (Figure 6E, S6D), which explains the elevated GSK3β S9-phosphorylation. These findings indicate that DISC1-Δ3 is unable to bind to Girdin and therefore, it inhibits GSK3β activity indirectly through the Girdin-AKT pathway, resulting in increased Wnt/β-catenin signaling (Figure 6F schematic diagram).

We further confirmed the hyperactivation of Wnt/β-catenin pathway in the OPCs, from the hippocampus of schizophrenia patients, by detecting an increased immunoreactivity of Wnt downstream gene RNF43 (181.4 ± 30.5% increase, Figure 6G-H). This is consistent with a recent finding that upregulation of RNF43 specifically in OPCs correlates with hyperactivated Wnt-signaling in injuries[32,33]. In this regard, we postulate that the DISC1-Δ3 in OPCs mediates a 'gain-of-function' to promote the hyperactivity of the Wnt/β-catenin signaling pathway in schizophrenia brains.

However, the morphological changes in OPCs cannot be achieved either *in vivo* or *in vitro* by OPC-specific conditional deletion of the obligate Wnt pathway inhibitor, adenomatous polyposis coli (APC) (Figure S6E-F). This suggests that Wnt/β-catenin pathway is probably not involved in generation of the DISC1-Δ3 OPCs morphological phenotype.

Wnt-driven Wif1 overexpression impairs synaptic formation

As Wnt/β-catenin pathway activity governs the expression of downstream genes in multiple cellular processes[34], we investigated how hyperactive Wnt signaling in DISC1-Δ3 OPCs affects synaptic formation. Differential expression analysis showed that DISC1-Δ3 altered the expression of several secretory protein-coding genes (Figure S7A-B), especially Wif1 (420.1 ± 21.4-fold increase, Figure 7A), which is a downstream target of Wnt and an inhibitor of the Wnt pathway[35]. Recently, it has been proposed that upregulated Wif1 forms part of a negative feedback mechanism to counteract the excessive activities of the Wnt signaling pathway in OPCs[36].

Increased expression of Wif1 was detected by immunostaining, ELISA, western blot, and qPCR (55.2 ± 21.4%, 23.3 ± 3.9%, 100.2 ± 38.9%, and 500.0 ± 163.1% increase, respectively, Figure 7B-E, S7C). Consistent with our findings in DISC1-Δ3 mice, WIF1 intensity was significantly increased by 111.4 ± 34.5% in the hippocampus of schizophrenia patients when compared to that in the age-matched healthy controls (Figure 7F), which is in agreement with previous observations that WIF1 is altered in schizophrenia postmortem brains[37,38].

Since Wif1 is a secreted factor, the overproduction of Wif1 in OPCs may affect other Wnt-dependent processes in adjacent neurons, such as synaptogenesis[39]. To address this question, we measured the

activation of Wnt signaling pathway in acutely isolated neurons from P10 DISC1-Δ3 and non-CreERT wildtype mice. We found that the target genes of the non-canonical Wnt pathways[40] were downregulated in the neurons from DISC1-Δ3 mice, whereas the canonical Wnt/β-catenin pathway remains unchanged (Figure 7G). Next, we treated primary wildtype hippocampal neurons with the synaptogenic Wnt ligand Wnt7a[41] in the presence of Wif1 protein. Wif1 treatment resulted in 80.8 ± 10.6% reduction in the number of $SYN1^+$ synaptic puncta compared to Wnt7a-treatment alone (Figure 7H). This was accompanied by a decrease in Wnt/Ca^{2+} signaling elements: 55.9 ± 5.0% reduction in CaMK II phosphorylation and suppressed mRNA expression of non-canonical Wnt target genes (Figure 7I-J, S7D). Similar changes occur in neurons from DISC1-Δ3 mice, which agrees with previous studies that the canonical and non-canonical Wnt pathways regulate synaptogenesis[42-44]. Therefore, our data suggest that the overproduction of Wif1 protein from DISC1-Δ3 OPCs results in the inhibition of synaptogenesis mediated by non-canonical Wnt pathway.

Downregulation of Wif1 rescues synaptic defects and behavioral abnormalities in DISC1-Δ3 mice

To further verify whether manipulating Wif1 expression can rescue synaptic defects and behavioral abnormalities in DISC1-Δ3 mice, we knocked down Wif1 in the DISC1-Δ3 OPCs by microinjecting Wif1 shRNA retrovirus into the hippocampus[45]. The infection efficiency was confirmed by the co-expression of retrovirus-driven GFP and the $NG2^{creERT}$-driven tdTomato (Figure S8A). The infection specificity for oligodendroglial cells was validated by co-labeling of GFP^+ with $NG2^{creERT}$:$tdTomato^+$ (82.13 ± 1.45%) and $PDGFR\alpha^+$ (45.19 ± 1.11%), but rarely with the markers of neurons (5.03 ± 0.38%), microglial cells (5.44 ± 0.67%), astrocytes (0.69 ± 0.69%), and pericytes (1.33 ± 0.67%) (Figure S8A), which is consistent with previous observations[45]. Western blot and ELISA showed that Wif1 knockdown decreased Wif1 protein levels in the hippocampus (Figure S8B-C), and improved synaptic formation by 35.4±12.7%, as judged by the $SYN1^+$ puncta quantification (Figure 8A-B). However, Wif1 knockdown did not change the total number of oligodendroglial lineage cells, oligodendroglial differentiation, degree of myelination, or OPC morphology (Figure S8D-H).

Subsequently, we conditionally knocked out Wif1 in the OPCs of DISC1-Δ3 mice (Figure S8I). This did not change the number, differentiation, or hypertrophic morphology of OPCs (Figure S8J-N). However, such conditional knockout increased synaptogenesis as evidenced by a 47.1 ± 9.8% increase in $SYN1^+$ puncta (Figure 8C-D). In particular, we observed an increase in the number of vGLUT1 labeled excitatory synapses while the number of vGAT-positive inhibitory synapses remained unchanged (Figure 8C-D). Furthermore, Wif1 knockout reversed neuronal activity alterations, as demonstrated by restored sEPSC in hippocampal neurons (Figure 8E-G). Wif1 conditional knockout also mitigated schizophrenia-like behavioral abnormalities such as increased prepulse inhibition and decreased center distances in the open field test in DISC1-Δ3 mice, (Figure 8H-I), suggesting an improvement in behavioral abnormalities[46].

Taken together, our results from the DISC1-Δ3 mouse model confirm that Wnt-hyperactivation in the OPCs can disrupt synapse formation and initiate the pathogenesis of schizophrenia by overproduction of Wnt inhibitor Wif1. As a result, the downregulation of Wif1 in DISC1-Δ3 OPCs restored synaptic formation and improved neuronal function.

Discussion

We identified hypertrophic OPCs as a new hallmark of schizophrenic brains in both human patients and mouse model, provided compelling evidence that expression of DISC1 exon 3 splicing variant solely in OPCs is sufficient to suppress synaptogenesis, and presented a novel mechanism by which the onset of schizophrenia related to OPCs is mainly driven by the overproduction of Wif1, a Wnt-pathway inhibitor, in response to the hyperactivation of Wnt/β-catenin signaling in DISC1-Δ3 OPCs.

Evidence gathered previously suggests that myelin defects contribute to pathophysiology of schizophrenia[7]. However, several DTI studies on young patients showed no changes in white matter at the onset of disease[8-11]. This contradicts the current hypothesis postulating that schizophrenic phenotypes originate from myelin defects, and hints at an alternative possibility that myelin abnormalities may not be necessarily responsible for the onset of disease in young schizophrenia patients, but develop as the disease progresses[8-11]. Our *in-vivo* and *in-vitro* findings demonstrate that abnormal OPC function initiates neuronal malfunction. In particular, expression of a single gene variant DISC1-Δ3 in the OPCs is sufficient to trigger the onset of schizophrenia-related pathological changes, which may explain the results of previous imaging studies. Schizophrenia is usually diagnosed between late adolescence and early thirties[47,48], when myelination is still ongoing[49,50]. Any abnormal activation of Wnt/β-catenin pathway in OPCs within this age may affect their differentiation and hinder myelination[51,52]. Indeed, our findings in schizophrenia patients and mouse model show that Wnt-signaling elements in the OPCs are hyperactive especially at the initiation of schizophrenia-like pathology in mice, suggesting that defects in myelination may follow later when disease evolves[9,10]. Overall, early changes in OPCs, including hypertrophy and Wnt-signaling hyperactivation, may either initiate or contribute to the onset of schizophrenia.

Our study further corroborates the multi-functional role of OPCs in the central nervous system (CNS). In other neurological disorders, such as multiple sclerosis, hypoxic-ischemic encephalopathy, and psychiatric diseases, OPCs not only contribute to aberrant myelin formation[33,51], but are also involved in the regulation of blood-brain barrier integrity[36], CNS immune regulation[53,54] and the behavioral outcomes[55,56]. In the present study, we generated a novel transgenic mouse strain to model the heterozygous DISC1 exon 3 splicing in patients with schizophrenia, and provided new evidence that such manipulation of DISC1 gene transcription exclusively in OPCs causes OPC hypertrophy, disrupts the formation of $vGLUT1^+$ excitatory synapses, and initiate schizophrenia-like symptoms.

Mechanistically, we found that DISC1-Δ3 significantly enhances the activation of Wnt/β-catenin pathway by regulating GSK3β, the Wnt/β-catenin pathway inhibitor, both directly and indirectly. The DISC1-Δ3 protein retains GSK3β binding region, and therefore can directly interact with GSK3β to suppress its Y216 residue autophosphorylation and catalytic activity[28,29], although the underlying mechanism requires further scrutiny. On the other hand, it has been reported that GSK3β S9 can be phosphorylated by several protein kinases, such as AKT (PKB)[31,57]. While AKT activity can be suppressed by DISC1 due to its competitive binding to Girdin, the AKT co-activator[30], we found that the AKT pathway is activated by DISC-Δ3 variant lacking the Girdin binding region, thus resulting in an indirect enhancement of GSK3β S9 phosphorylation. By analyzing both direct and indirect regulation, we provided new insights into how DISC1-Δ3 stabilizes β-catenin and promotes Wnt/β-catenin signaling in the OPCs, which may act as a starting point of schizophrenia pathogenesis. This new mechanism is in agreement with observations showing altered Wnt pathway genes such as GSK3β, WIF1, as well as AKT1in schizophrenia postmortem brains[37,38,58]. Notably, manipulating Wif1 production alone improves synaptogenesis and mitigates schizophrenia-like behaviors in DISC-Δ3 mice. Consequently, DISC-Δ3 represents a perspective target for novel treatment strategies. Since DISC1 can also regulate neurogenesis, neurite outgrowth, and synaptic plasticity, which are all involved in the pathogenesis of schizophrenia[29,30,59,60], future studies may be used to understand the contribution of DISC1-Δ3 in other cell types to the schizophrenia phenotype.

Notably, OPCs hypertrophy is not linked to the overactivation of Wnt/β-catenin pathway in DISC1-Δ3 mice, as our experiments, as well as previous studies, failed to induce such morphological change by increasing Wnt/β-catenin signaling pathway activity. Changes in OPCs morphology may be caused by DISC1 acting as a scaffolding protein, with the DISC1-Δ3 variant changing the cytoskeletal dynamics through AKT/mTOR signaling[30,61]. Such possibility was supported by our KEGG pathway analysis. Alternatively, prolonged inhibition of GSK3β can cause cell hypertrophy[62]. Be it as it may, morphological changes correlate with the functional changes in OPCs, and thus OPCs hypertrophy may be used as a histological hallmark for early-stage schizophrenia.

In conclusion, our findings provide new evidence on the mechanism of how pathological OPCs initiate schizophrenia in genetically susceptible individuals. Targeting Wif1 in OPCs may open a new direction in developing effective therapeutic strategies for schizophrenia.

Declarations

Acknowledgments:

National Nature Science Foundation of China (NSFC 32070964 and 31871045 to J.N.; 31970921 and 31921003 to L.X.; 81971309 and 32170980 to C.Y.). National Key Research and Development Program of China (2021ZD0201703 to J.N. and L.X.). Guangdong Basic and Applied Basic Research Foundation (2019A1515011333 to C.Y.). Shenzhen Fundamental Research Program (JCYJ20190809161405495,

JCYJ20210324123212035 and RCYX20200714114644167 to C.Y.). Zhejiang Provincial Natural Science Foundation of China (LR19C090001 to Y.C.).

Author contributions:

Conceptualization: J.N., L.X. and A.V. Methodology: J.N., L.X., C.Y. and Y.C. Investigation: J.N., G.Y., Y.S., Y.C., G.Y., Y.S., B.Y., G.C., C.Y., X.W., Y.W., X.C., S.W., Q.W., X.H. and J.N. Visualization: J.N., G.Y., Y.S., Y.C., G.Y., Y.S. and B.Y. Funding acquisition: J.N., L.X., C.Y. and Y.C. Project administration: J.N. and L.X. Supervision: J.N. and L.X. Writing – original draft: J. N., C.Y. and Y.S. Writing – review & editing: J. N., C.Y., H. C., F. M. and L.X and A.V.

Competing interests

The authors declare that they have no competing interests.

Materials And Methods

Mice

All mice were maintained on a 12 h/12 h light/dark cycle with free access to food and water. All animal procedures were conducted under institutional guidelines and protocols approved by the animal welfare and ethics committee of the third military medical university at Chongqing. The C57BL/6 wild-type mice were purchased from the university animal breeding center.

$NG2^{CreERT}$ mice have been described previously [63] . R26-LSL-tdTomato mice (The Jackson Laboratory, 007908) or mT/mG mice (The Jackson Laboratory, 007676) were crossed with the $NG2^{CreERT}$ mice to validate the oligodendroglial-specific targeting and to visualize cell morphology.

The DISC1 exon3-flox and Wif1-flox mice were generated de novo using the CRISPR-Cas9 system to insert loxP sites franking DISC1 exon3 and Wif1, respectively, in C57BL/6 mouse zygotes, which were then transferred to pseudo-pregnant CD1 mice at the blastocyst stage. These procedures were performed by Gempharmatech. Co., Ltd, China. The mice were then crossed with $NG2^{CreERT}$ mice to generate $NG2^{CreERT}$: $DISC1^{exon3\ fl/+}$ (DISC1-Δ3) or $NG2^{CreERT}$: $DISC1^{exon3\ fl/+}$: $Wif1^{fl/fl}$ conditional knockout (cKO) mice; or crossed with PLP^{CreERT} mice [64] to generate PLP^{CreERT}: $DISC1^{exon3\ fl/+}$ (DISC1-Δ3 OL) cKO mice.

$PDGFR\alpha^{creER}$ mice [65] or $Olig2^{cre}$ mice [66] were crossed with $APC^{fl/fl}$ mice [67] to over-activate the Wnt pathway in OPCs.

To induce Cre-mediated recombination, the mice were given tamoxifen (10 mg/kg, Sigma-Aldrich, T5648) force-fed for 4 consecutive days (P4-P7) or 6 consecutive days (P40-P45).

Behavioral Tests

Prepulse inhibition test: the acoustic startle response was measured with automated startle chambers (MED ASSOCIATES, INC, MED-ASR-PRO1) as previously described [68] . Briefly, each test began with a

habituation phase (10 min with a constant 65 dB background noise), Startle responses to a 120 dB auditory stimulus were measured for a period of 40 ms. The test session consisted of 45 trials with no stimulus (background white noise only), 120 dB pulse of 40 ms duration, or 120 dB pulse preceded 40 ms by a 75 dB pulses of 20 ms in duration. Trials were given in random order with variable intervals (20–60 s) between each trial. Percentage of prepulse inhibition (%PPI) was calculated as %PPI = 100 × [(pulse alone score) − (prepulse + pulse score)]/pulse alone score.

Open field test: The open field test was performed to determine locomotor activity and anxiety-like behavior, mice were placed in the center of an open field box (50 × 50 × 50 cm) (Biowill, Shanghai, China), and their activity was recorded for 20 min. The time and distances traveled in the center zone, as well as the total distances traveled, were measured.

Cliff avoidance reaction test: This test was performed to evaluate the impulsive behavior as described previously [69] . A round platform (diameter of 16 cm; thickness of 2 cm) was set up at the height of 50 cm, and each mouse was then gently placed on the platform and the duration (20 min) that it remained on the platform was recorded.

Social interaction test: The test was performed as described previously [70] . Briefly, the test was divided into two phases, each of which lasted 10 min. In the first phase, the test mice were placed in the middle of the box and allowed to move freely in the chamber for 10 min while two empty wire cages were placed in the left and right of the chamber. In the second phase, a C57BL/6J stranger mouse that had never been exposed to the test mice was placed in one wire cage, the test mouse was allowed to freely explore the chamber for 10 min. To determine whether the mouse was susceptible or resilient, the time spent in the interaction zone and the time spent in the no interaction zone were recorded.

Novel object recognition Test: The experimental apparatus was an open-field chamber (25 cm × 25 cm × 40 cm). Mice were individually habituated in the empty chamber for 2 days (5 min per day) before testing. During the test, two identical objects were placed into the chamber and the mice were allowed to explore freely for 5 min. Two hours later, one of the objects was replaced by a novel object, the mouse was re-introduced into the apparatus and recorded 5min, a ratio of the amount of time spent in exploring the novel object over the total time spent in exploring both objects was measured.

Hippocampus brain slice preparation and electrophysiological recordings

The method has been described previously [71] . Animals were rendered unconscious by 4% isoflurane in the air. Brains were removed and placed for 30s in an ice-cold and oxygenated artificial ACSF containing 125 mM NaCl, 2.5 mM KCl, 25 mM $NaHCO_3$, 1.25 mM NaH_2PO_4, 1 mM $MgCl_2$, 1 mM $CaCl_2$, 25 mM glucose, 1 mM sodium pyruvate and continuously gassed with 95% O_2 and 5% CO_2. Transverse slices (300 µm) were cut on a vibratome (Leica VT1200S), incubated in ACSF at 32 ℃ with oxygenated (95% O_2 and 5% CO_2) at least 30 min and stored in a recording solution at room temperature. For hippocampus neuron spontaneous excitatory postsynaptic currents (sEPSCs) and inhibitory postsynaptic currents (sIPSCs) recording, whole-cell patch-clamp recordings were made with borosilicate glass pipettes (PC-100, Narishige; 5-6 MΩ) in voltage-clamp mode and at the holding potential (HP) of –70 mV (sEPSC) and 0mV (sIPSC). Recording pipettes were filled with internal solution of the following composition (mM): 125 mM Cs-methane sulphonate, 8 mM NaCl, 2 mM Mg-ATP, 0.3 mM Na_3-GTP, 0.3 mM EGTA, 10 mM HEPES and 10 mM Na-phosphocreatine (pH = 7.25). Cells were visualized with

infrared optics on an upright microscope (BX51WI, Olympus). A MultiClamp 700B amplifier and pCLAMP10 software were used for electrophysiology (Axon Instruments).

Primary cell cultures

OPCs and other brain cell types were isolated from cerebral hemispheres of P7 mouse pups by immunopanning as previously described [15] . Immunopanning antibodies used were: OPC, Pdgfrα antibody (Abcam, ab96569); microglia, CD45 antibody (BD Pharmingen™, ab550539); astrocyte, Integrin beta 5 antibody (eBioscience, 14-0497-82); neuron, p75 NGF receptor antibody (Abcam, ab52987).

These purified mouse OPCs were cultured in poly-D-lysine-coated 10 cm dishes or 24-well plates with coverslips for experiments. In the OPC culture medium, PDGF-AA (10ng/ml, Peprotech, 100-13A) was used to stimulate OPC proliferation and was removed from the culture medium to induce OPC differentiation. The cells on coverslips were fixed for immunostaining, proteins were collected for Western blot. The purified mouse OPCs were cultured for 4 days for cultured medium collection. The collected medium was filtered with a 0.22 μm filter (Millipore), then collected as the conditioned medium for downstream experiments or stored at -80°C.

For primary neuronal culture, mouse hippocampal neurons were isolated from E15-17 mouse embryos. Cells were resuspended in Neurobasal medium with B27, GlutaMax, and 1 mM HEPES, supplemented with 10% FBS, filtered through a 70 μm cell strainer, and plated onto poly-L-lysine coated coverslips. The medium was replaced with neuron culture medium the next day, and AraC (10 μM) was added to the cell culture to kill proliferating cells on day 2, and then replaced with neuron culture medium again on day 3.

For OPC-neuron co-culture, the purified OPCs were seeded onto primary neurons in 24-well plates on day 9 and maintained in OPC-neuron culture medium (50% neuron culture medium and 50% OPC medium without PDGF-AA).

For neuron treatments, Wnt7a (100ng/ml, Peprotech, 120-31), Wif1 (1ug/ml, Abcam, ab208465), or Wnt7a with Wif1 were used to incubate with primary cultured neurons in 24-well plates on day 9 for 24 hours. PBS treatment was used as the control. To test the effects of OPC-conditioned medium on neurons, primary cultured neurons were treated with conditioned medium (25% fresh medium+ 75% conditioned medium) for 24 hours.

Immunohistochemistry

The method has been described previously [36] . Primary antibodies used were: Rabbit anti-NeuN (Abcam, ab177487), Rabbit anti-c-Fos (CST, 2250S), Rabbit anti-BLBP (Abcam, ab32423), Rabbit anti-NG2 (Millipore, MAB5320), Rat anti-PDGFRα (BD Biosciences, 558774), Rabbit anti-Olig2 (Millipore, AB9610), Mouse anti-CC1 (Millipore, OP80), Rat anti-MBP (Millipore, MAB386), Rabbit anti-Iba1 (Wako, 019-19741), Rabbit anti-Ki67 (Thermo, MA514520), Goat anti-GFP (Abcam, ab5450), Rat anti-PDGFRβ (Invitrogen, 14-1402-81), Rabbit anti-Synapsin1 (CST, #5297), Rabbit anti-Homer1(Synaptic

Systems,#160003), Mouse anti-Vgat (Millipore,#AB5062P), Guinea pig anti-VGLUT1 (Millipore, #AB5905), Chicken anti-MAP2 (Millipore, AB5543), Lectin (Vector Laboratories, Inc. DL-1174), Mouse anti-Fibrinogen (Abcam, ab58207). Images were captured using VS200 Research Slide Scanner (Olympus), FV3000 confocal microscope (Olympus), SpinSR confocal microscope (Olympus), or Axio Imager M2 with the apotome system (Zeiss).

RNA-seq

RNA-seq experiments were performed on freshly isolated OPCs from the DISC1-Δ3 and WT mice at P7. OPCs were isolated by immunopanning as described previously [15] . RNA was extracted from the isolated cells by Trizol (Thermo) according to the manufacturer's protocol. RNA-seq was performed by the Beijing Genomics Institute (BGI). Differential expression analysis was performed using DESeq2.

ELISA

To examine the concentrations of Wif1 proteins in brain lysates, mouse Wif1 Elisa Kit (CUSABIO, CSB-EL026113MO) was used according to the manufacturer's instructions. The OD values were determined by measuring the absorbance at 450 nm using a microplate reader (Bio-RAD, Model 680). Independent experiments were performed in triplicates.

RT-qPCR

Total RNA was isolated by TRIZOL® combined with the RNeasy Plus Mini Kit (Qiagen, 74134) according to the manufacturer's protocol. cDNA was synthesized from 1 μg of total RNA. Quantitative polymerase chain reaction (qPCR) was performed with the Real-time PCR Detection System (Roche) and FastStart Universal SYBR® Green Master (Roche, 04913850001). RT-qPCR primer sequences for DISC1 variant expression analyses were listed as follows: DISC1 full (forward 5′-GAGGATGGCGATTACGATACTG-3′, reverse 5′-AGAGCAGGTTGCTGTGAAG-3′, span from exon3 to exon4); DISC1-Δ3 (forward 5′-GAGCAGAGACATTGAGACAGAG-3′, reverse 5′-CTGCCAGGTAACCCAAGAA-3′, span from exon2 to exon 2-exon4 boundary); DISC1-Δ7/8 (forward 5′-CAGGAGGAAGCTGCTTCTCC-3′, reverse 5′-CAGGAACATCTCTAGCCCTTC-3′, span from exon5 to exon6-exon9 boundary).

Western blot

To determine the protein expression pattern of DISC1, Wif1, p-GSK-3β, GSK-3β, p-β-catenin, and β-catenin in OPCs and brain tissue, western blot analysis was performed. Briefly, 40-80 μg of protein were separated by 10% SDS-PAGE and then electrophoretically transferred to nitrocellulose membrane. Membranes were probed by antibodies including rabbit anti-DISC1 (Abcam, ab192258), rabbit anti-Wif1 (Abcam, ab155101), mouse anti-p-GSK-3β (Ser9) (CST, #14630), rabbit anti-GSK-3β (CST, #9315), rabbit anti- p-β-catenin (Ser33/37/Thr41) (CST, #9561), rabbit anti-β-catenin (CST, #8480), rabbit anti-p-SAPK/JNK (Thr183/Tyr185) (CST, #4668), rabbit anti-SAPK/JNK (CST, #9252), rabbit anti-p-CaMKII(Thr286) (CST, #12716), rabbit anti-CaMKll alpha (Abcam, ab92332) and mouse anti-β-actin (Beyotime, AF0003). Protein bands were visualized by chemiluminescence (ECL Plus, GE Healthcare) after incubation with HRP-conjugated secondary antibodies. Images were captured by ChampChemi 610 Chemiluminescence Imaging System (Beijing Sage Creation, China). Protein band intensity was analyzed using the Image Pro Plus software.

Wif1 shRNA Retrovirus and Stereotaxic surgery

To silence *Wif1* expression in vivo, three shRNA sequences targeting different sites of *Wif1* mRNA were designed, and a scrambled shRNA target sequence was designed as a negative control. The target sequences were: shRNA1, CCAACTGTCAATGTCCCTT; shRNA2, GCTCAACCACCTGCTTTAA; shRNA3, GGGATCCACCTGAATCCAA. The shRNA sequences were inserted into the previously described retrovirus vector [45] . Using stereotaxic techniques, pROV-U6-shRNA1(Wif1)-EF1A(S)-EGFP-3Flag [pROV-U6-shRNA (Scramble)-EF1A(S)-EGFP-3Flag as negative control] was injected bilaterally into the hippocampus CA1 of the P10 mouse at the following coordinates: 1.5 mm posterior to bregma, 0.8 mm from the midline and 1.8mm ventral to the surface of the skull. The total volume injected was 1 µL ($1.5e^5$ TU). The needle was left in place for an additional 10 min after injection. Two days post retrovirus injection, mice were perfused with 4% buffered paraformaldehyde.

Human schizophrenia tissues and immunohistochemical staining

Human schizophrenia and healthy comparable post-mortem tissue slides were provided by the National Health and Disease Human Brain Tissue Resource Center at Zhejiang University in China (S2019017). All human tissues were collected following fully informed consent by the donors via a prospective donor scheme following ethical approval by the Human Ethics committee of Zhejiang University School of Medicine (#2020-005). Cases assessed are described in Figure S1A.

The immunohistochemical technique has been described previously; with some modifications [36] . Briefly, the human paraffin tissue sections were deparaffinized by immersion in fresh xylene twice for 10 min each, rehydrated with a grade descending series of ethanol concentrations, and treated with 3% H_2O_2 for 10 min at RT to eliminate the endogenous peroxidase. Antigen retrieval was performed in citrate buffer (pH 6.0) and microwaved at high power for 2 min. After blocking with 5% bovine serum albumin and 0.2% Triton X-100 for 1 hour at room temperature, the samples were incubated with primary antibodies: rabbit anti-NG2 (Millipore, AB5320), rabbit anti-RNF43 (Abcam, ab217787), rabbit anti-OLIG2 (Millipore, AB9610), rabbit anti-WIF1 (Abcam, ab186845) overnight at 4 ℃. Next, biotinylated goat anti-rabbit IgG (BOSTER, SA2002, China) was applied at 37°C for 30 min, and an additional incubation of slides in streptavidin- peroxidase complex (BOSTER, SA2002, China) was performed for 30 min at 37°C. Then, 3,3′-diaminobenzidine (Abcam, ab64238) was used for chromogenic detection. The frozen sections of human tissues were blocked with 5% bovine serum albumin and 0.2% Triton X-100 for 1 hour at room temperature, followed by being labeled with primary antibody rabbit anti-NG2 (Millipore, AB5320) overnight at 4℃. The immunoreaction was visualized by DAB. Images were captured by using VS200 Research Slide Scanner (Olympus) or Axio Imager M2 with the apotome system (Zeiss).

Quantification methods

Images captured with the VS200 Research Slide Scanner and FV3000 confocal microscope were used to quantify cell numbers. To quantify positive cell numbers, cell counting was conducted on nine randomly chosen fields for each sample using an Image Pro Plus image analysis system. The number of cells in a fixed area in the CA1 region was quantified manually. The positive cell coverage was calculated as: positive cell coverage = positive area / the number of cells in a fixed area. The Sholl analysis was performed using a Fiji Sholl Analysis plugin described previously [72] . This measurement was only done for OPCs in which the cell processes were clearly seen. Quantification of synapse puncta was done using images captured by the FV3000 confocal microscope, which was then analyzed using the Fiji software. The fluorescent intensity and Western-blot positive band, the positive areas were automatically selected

in image-Pro Plus 5 software. The areas of interest (AOI) were separated by setting the threshold at least two times the background.

Statistical analysis

Statistical significance between groups was determined using the GraphPad Prism software 9.0 (GraphPad Software, San Diego, CA, USA). Data were presented as means ± standard deviation (SD). Fold changes reported in the text are (mean difference ± SEM of difference) % compared to the controls. The unpaired t-test was used to determine the significance between two experimental groups, while one-way analysis of variance (ANOVA) was used to determine statistical significance when comparing multiple groups. All statistical tests were two-tailed. *p*-values less than 0.05 were considered statistically significant. Significant statistical results are indicated as: * $p < 0.05$, ** $p < 0.01$, *** $p < 0.001$, **** $p < 0.0001$. No statistical methods were used to pre-determine sample sizes but our sample sizes are similar to those reported in the previous publications (Niu et al., 2019). Data distribution was assumed to be normal, but this was not formally tested. All experiments were performed at least 3 times, and the findings were replicated in individual mice and cell cultures in each experiment.

Data and materials availability: All data are available in the main text or the supplementary materials. RNA-seq data have been deposited in the NCBI GEO under the accession number GSE183341.

References

1. Kahn, R.S.*, et al.* Schizophrenia. *Nature reviews. Disease primers* **1**, 15067 (2015).

2. Vos, T.*, et al.* Global, regional, and national incidence, prevalence, and years lived with disability for 328 diseases and injuries for 195 countries, 1990–2016: a systematic analysis for the Global Burden of Disease Study 2016. *The Lancet* **390**, 1211-1259 (2017).

3. World-Health-Organization. Schizophrenia. (Geneva, 2022).

4. Cetin-Karayumak, S.*, et al.* White matter abnormalities across the lifespan of schizophrenia: a harmonized multi-site diffusion MRI study. *Mol Psychiatry* **25**, 3208-3219 (2020).

5. Maas, D.A., Vallès, A. & Martens, G.J.M. Oxidative stress, prefrontal cortex hypomyelination and cognitive symptoms in schizophrenia. *Translational psychiatry* **7**, e1171 (2017).

6. Mauney, S.A., Pietersen, C.Y., Sonntag, K.C. & Woo, T.W. Differentiation of oligodendrocyte precursors is impaired in the prefrontal cortex in schizophrenia. *Schizophrenia research* **169**, 374-380 (2015).

7. Takahashi, N., Sakurai, T., Davis, K.L. & Buxbaum, J.D. Linking oligodendrocyte and myelin dysfunction to neurocircuitry abnormalities in schizophrenia. *Progress in neurobiology* **93**, 13-24 (2011).

8. Foong, J.*, et al.* Investigating regional white matter in schizophrenia using diffusion tensor imaging. *Neuroreport* **13**, 333-336 (2002).

9. Mighdoll, M.I., Tao, R., Kleinman, J.E. & Hyde, T.M. Myelin, myelin-related disorders, and psychosis. *Schizophrenia research* **161**, 85-93 (2015).

10. Price, G., Bagary, M.S., Cercignani, M., Altmann, D.R. & Ron, M.A. The corpus callosum in first episode schizophrenia: a diffusion tensor imaging study. *Journal of neurology, neurosurgery, and psychiatry* **76**, 585-587 (2005).

11. Steel, R.M.*, et al.* Diffusion tensor imaging (DTI) and proton magnetic resonance spectroscopy (1H MRS) in schizophrenic subjects and normal controls. *Psychiatry research* **106**, 161-170 (2001).

12. Katsel, P.*, et al.* Expression of mutant human DISC1 in mice supports abnormalities in differentiation of oligodendrocytes. *Schizophrenia research* **130**, 238-249 (2011).

13. Vasistha, N.A.*, et al.* Familial t(1;11) translocation is associated with disruption of white matter structural integrity and oligodendrocyte-myelin dysfunction. *Mol Psychiatry* **24**, 1641-1654 (2019).

14. Lake, B.B.*, et al.* Integrative single-cell analysis of transcriptional and epigenetic states in the human adult brain. *Nature biotechnology* **36**, 70-80 (2018).

15. Zhang, Y.*, et al.* An RNA-sequencing transcriptome and splicing database of glia, neurons, and vascular cells of the cerebral cortex. *The Journal of neuroscience : the official journal of the Society for Neuroscience* **34**, 11929-11947 (2014).

16. Millar, J.K.*, et al.* Disruption of two novel genes by a translocation co-segregating with schizophrenia. *Human molecular genetics* **9**, 1415-1423 (2000).

17. Callicott, J.H.*, et al.* Variation in DISC1 affects hippocampal structure and function and increases risk for schizophrenia. *Proc Natl Acad Sci U S A* **102**, 8627-8632 (2005).

18. Nakata, K.*, et al.* DISC1 splice variants are upregulated in schizophrenia and associated with risk polymorphisms. *Proc Natl Acad Sci U S A* **106**, 15873-15878 (2009).

19. Newburn, E.N.*, et al.* Interactions of human truncated DISC1 proteins: implications for schizophrenia. *Translational psychiatry* **1**, e30 (2011).

20. Provenzano, F.A.*, et al.* Hippocampal Pathology in Clinical High-Risk Patients and the Onset of Schizophrenia. *Biological psychiatry* **87**, 234-242 (2020).

21. Ma, L.*, et al.* Cloning and characterization of Disc1, the mouse ortholog of DISC1 (Disrupted-in-Schizophrenia 1). *Genomics* **80**, 662-672 (2002).

22. Owen, M.J., Sawa, A. & Mortensen, P.B. Schizophrenia. *Lancet (London, England)* **388**, 86-97 (2016).

23. Jones, C.A., Watson, D.J. & Fone, K.C. Animal models of schizophrenia. *British journal of pharmacology* **164**, 1162-1194 (2011).

24. Gao, R. & Penzes, P. Common mechanisms of excitatory and inhibitory imbalance in schizophrenia and autism spectrum disorders. *Curr Mol Med* **15**, 146-167 (2015).

25. Canitano, R. & Pallagrosi, M. Autism Spectrum Disorders and Schizophrenia Spectrum Disorders: Excitation/Inhibition Imbalance and Developmental Trajectories. *Front Psychiatry* **8**, 69 (2017).

26. Azim, K., Rivera, A., Raineteau, O. & Butt, A.M. GSK3beta regulates oligodendrogenesis in the dorsal microdomain of the subventricular zone via Wnt-beta-catenin signaling. *Glia* **62**, 778-779 (2014).

27. Cross, D.A., Alessi, D.R., Cohen, P., Andjelkovich, M. & Hemmings, B.A. Inhibition of glycogen synthase kinase-3 by insulin mediated by protein kinase B. *Nature* **378**, 785-789 (1995).

28. Lochhead, P.A.*, et al.* A chaperone-dependent GSK3beta transitional intermediate mediates activation-loop autophosphorylation. *Molecular cell* **24**, 627-633 (2006).

29. Mao, Y.*, et al.* Disrupted in schizophrenia 1 regulates neuronal progenitor proliferation via modulation of GSK3beta/beta-catenin signaling. *Cell* **136**, 1017-1031 (2009).

30. Kim, J.Y.*, et al.* DISC1 regulates new neuron development in the adult brain via modulation of AKT-mTOR signaling through KIAA1212. *Neuron* **63**, 761-773 (2009).

31. Jope, R.S. & Johnson, G.V. The glamour and gloom of glycogen synthase kinase-3. *Trends in biochemical sciences* **29**, 95-102 (2004).

32. Fancy, S.P.*, et al.* Parallel states of pathological Wnt signaling in neonatal brain injury and colon cancer. *Nature neuroscience* **17**, 506-512 (2014).

33. Niu, J.*, et al.* Oligodendroglial ring finger protein Rnf43 is an essential injury-specific regulator of oligodendrocyte maturation. *Neuron* **109**, 3104-3118.e3106 (2021).

34. Wodarz, A. & Nusse, R. Mechanisms of Wnt signaling in development. *Annual review of cell and developmental biology* **14**, 59-88 (1998).

35. Hsieh, J.C.*, et al.* A new secreted protein that binds to Wnt proteins and inhibits their activities. *Nature* **398**, 431-436 (1999).

36. Niu, J.*, et al.* Aberrant oligodendroglial-vascular interactions disrupt the blood-brain barrier, triggering CNS inflammation. *Nature neuroscience* **22**, 709-718 (2019).

37. Gregório, S.P.*, et al.* Polymorphisms in genes involved in neurodevelopment may be associated with altered brain morphology in schizophrenia: preliminary evidence. *Psychiatry research* **165**, 1-9 (2009).

38. Peng, Y., Xu, Y. & Cui, D. Wnt signaling pathway in schizophrenia. *CNS & neurological disorders drug targets* **13**, 755-764 (2014).

39. Park, M. & Shen, K. WNTs in synapse formation and neuronal circuitry. *The EMBO journal* **31**, 2697-2704 (2012).

40. Voloshanenko, O.*, et al.* β-catenin-independent regulation of Wnt target genes by RoR2 and ATF2/ATF4 in colon cancer cells. *Scientific reports* **8**, 3178 (2018).

41. Hall, A.C., Lucas, F.R. & Salinas, P.C. Axonal remodeling and synaptic differentiation in the cerebellum is regulated by WNT-7a signaling. *Cell* **100**, 525-535 (2000).

42. Cerpa, W.*, et al.* Wnt-7a modulates the synaptic vesicle cycle and synaptic transmission in hippocampal neurons. *J Biol Chem* **283**, 5918-5927 (2008).

43. Ciani, L.*, et al.* Wnt7a signaling promotes dendritic spine growth and synaptic strength through Ca²⁺/Calmodulin-dependent protein kinase II. *Proc Natl Acad Sci U S A* **108**, 10732-10737 (2011).

44. Simonetti, M.*, et al.* Wnt-Fzd signaling sensitizes peripheral sensory neurons via distinct noncanonical pathways. *Neuron* **83**, 104-121 (2014).

45. Chen, T.J.*, et al.* In Vivo Regulation of Oligodendrocyte Precursor Cell Proliferation and Differentiation by the AMPA-Receptor Subunit GluA2. *Cell Rep* **25**, 852-861 e857 (2018).

46. Marissal, T.*, et al.* Restoring wild-type-like CA1 network dynamics and behavior during adulthood in a mouse model of schizophrenia. *Nature neuroscience* **21**, 1412-1420 (2018).

47. Hollis, C. & Rapoport, J. Child and Adolescent Schizophrenia. in *Schizophrenia* 24-46 (2010).

48. McGrath, J., Saha, S., Chant, D. & Welham, J. Schizophrenia: a concise overview of incidence, prevalence, and mortality. *Epidemiologic reviews* **30**, 67-76 (2008).

49. Grydeland, H.*, et al.* Waves of Maturation and Senescence in Micro-structural MRI Markers of Human Cortical Myelination over the Lifespan. *Cerebral cortex (New York, N.Y. : 1991)* **29**, 1369-1381 (2019).

50. Miller, D.J.*, et al.* Prolonged myelination in human neocortical evolution. *Proc Natl Acad Sci U S A* **109**, 16480-16485 (2012).

51. Fancy, S.P.*, et al.* Dysregulation of the Wnt pathway inhibits timely myelination and remyelination in the mammalian CNS. *Genes Dev* **23**, 1571-1585 (2009).

52. Feigenson, K., Reid, M., See, J., Crenshaw, E.B., 3rd & Grinspan, J.B. Wnt signaling is sufficient to perturb oligodendrocyte maturation. *Mol Cell Neurosci* **42**, 255-265 (2009).

53. Falcao, A.M.*, et al.* Disease-specific oligodendrocyte lineage cells arise in multiple sclerosis. *Nat Med* **24**, 1837-1844 (2018).

54. Kirby, L.*, et al.* Oligodendrocyte precursor cells present antigen and are cytotoxic targets in inflammatory demyelination. *Nature communications* **10**, 3887 (2019).

55. Birey, F.*, et al.* Genetic and Stress-Induced Loss of NG2 Glia Triggers Emergence of Depressive-like Behaviors through Reduced Secretion of FGF2. *Neuron* **88**, 941-956 (2015).

56. Wang, Y.*, et al.* Reduced Oligodendrocyte Precursor Cell Impairs Astrocytic Development in Early Life Stress. *Advanced science (Weinheim, Baden-Wurttemberg, Germany)* **8**, e2101181 (2021).

57. Jensen, J., Brennesvik, E.O., Lai, Y.C. & Shepherd, P.R. GSK-3beta regulation in skeletal muscles by adrenaline and insulin: evidence that PKA and PKB regulate different pools of GSK-3. *Cellular signalling* **19**, 204-210 (2007).

58. Hallmayer, J. Getting our AKT together in schizophrenia? *Nature genetics* **36**, 115-116 (2004).

59. Miyoshi, K.*, et al.* Disrupted-In-Schizophrenia 1, a candidate gene for schizophrenia, participates in neurite outgrowth. *Mol Psychiatry* **8**, 685-694 (2003).

60. Tropea, D., Hardingham, N., Millar, K. & Fox, K. Mechanisms underlying the role of DISC1 in synaptic plasticity. *The Journal of physiology* **596**, 2747-2771 (2018).

61. Enomoto, A.*, et al.* Roles of disrupted-in-schizophrenia 1-interacting protein girdin in postnatal development of the dentate gyrus. *Neuron* **63**, 774-787 (2009).

62. Sugden, P.H., Fuller, S.J., Weiss, S.C. & Clerk, A. Glycogen synthase kinase 3 (GSK3) in the heart: a point of integration in hypertrophic signalling and a therapeutic target? A critical analysis. *British journal of pharmacology* **153 Suppl 1**, S137-153 (2008).

63. Zhu, X.*, et al.* Age-dependent fate and lineage restriction of single NG2 cells. *Development (Cambridge, England)* **138**, 745-753 (2011).

64. Doerflinger, N.H., Macklin, W.B. & Popko, B. Inducible site-specific recombination in myelinating cells. *Genesis* **35**, 63-72 (2003).

65. Kang, S.H., Fukaya, M., Yang, J.K., Rothstein, J.D. & Bergles, D.E. NG2+ CNS glial progenitors remain committed to the oligodendrocyte lineage in postnatal life and following neurodegeneration. *Neuron* **68**, 668-681 (2010).

66. Schüller, U.*, et al.* Acquisition of granule neuron precursor identity is a critical determinant of progenitor cell competence to form Shh-induced medulloblastoma. *Cancer cell* **14**, 123-134 (2008).

67. Robanus-Maandag, E.C.*, et al.* A new conditional Apc-mutant mouse model for colorectal cancer. *Carcinogenesis* **31**, 946-952 (2010).

68. Willott, J.F., Carlson, S. & Chen, H. Prepulse inhibition of the startle response in mice: relationship to hearing loss and auditory system plasticity. *Behavioral neuroscience* **108**, 703-713 (1994).

69. Yamashita, M.*, et al.* Impaired cliff avoidance reaction in dopamine transporter knockout mice. *Psychopharmacology* **227**, 741-749 (2013).

70. Han, Q.Q.*, et al.* Differential GR Expression and Translocation in the Hippocampus Mediates Susceptibility vs. Resilience to Chronic Social Defeat Stress. *Frontiers in neuroscience* **11**, 287 (2017).

71. Yang, Y.*, et al.* Ketamine blocks bursting in the lateral habenula to rapidly relieve depression. *Nature* **554**, 317-322 (2018).

72. Ferreira, T.A.*, et al.* Neuronal morphometry directly from bitmap images. *Nature methods* **11**, 982-984 (2014).

Figures

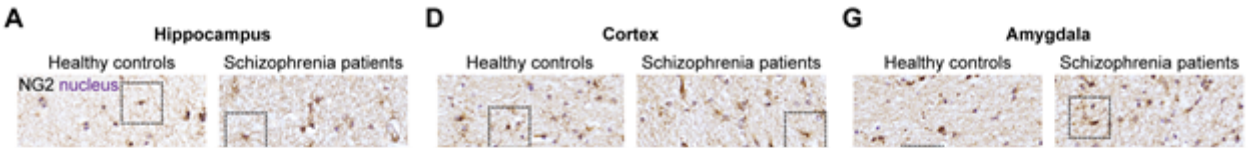

Figure 1

Hypertrophic OPCs in schizophrenia patients.

(A) Immunohistochemistry of NG2 in the paraffin-embedded cortical sections of healthy controls and schizophrenia patients. Arrowheads highlight $NG2^+$ OPCs.

(B) Quantification of $NG2^+$ OPC number in the cortex. n = 5 samples per group.

(C) Sholl analysis of $NG2^+$ OPC number in the cortex. n = 30 cells from samples per group.

(D) Immunohistochemistry of NG2 in the paraffin-embedded hippocampal sections of healthy controls and schizophrenia patients. Arrowheads highlight $NG2^+$ OPCs.

(E) Quantification of $NG2^+$ OPC number in the hippocampus. n = 5 samples per group.

(F) Sholl analysis of $NG2^+$ OPC number in the hippocampus. n = 30 cells from samples per group.

(G) Immunohistochemistry of NG2 in the paraffin-embedded amygdala sections of healthy controls and schizophrenia patients. Arrowheads highlight $NG2^+$ OPCs. Scale bar, 50 μm.

(H) Quantification of $NG2^+$ OPC number in the amygdala. n = 5 samples per group.

(I) Sholl analysis of $NG2^+$ OPC number in the amygdala. n = 30 cells from samples per group.

(J-L) Immunostaining and quantification of Olig2 in the hippocampus, cortex and amygdala. Scale bar, 50 μm. n = 5 samples per group.

Plots show individual data and mean ± SD, or mean ± SEM in Sholl analysis results. n.s., not significant, *p < 0.05, **p < 0.01, ****p <0.0001; paired t-test, or two-way ANOVA for Sholl analysis.

See also Figure S1.

Figure 2

Enhanced DISC1-Δ3 expression in the oligodendroglia phenocopies the hypertrophic OPC in patients.

(A) DISC1 exon 3 deletion induced by tamoxifen (TAM) in $NG2^{CreERT}$:$Disc1^{exon3\ flox}$ mice results in premature termination (blue lines highlight the coding region). Mice treated with TAM from P4 to P7 were analyzed at P23.

(B-C) Staining and quantification of Olig2 in the hippocampus. Scale bar: 50 μm. n = 4 mice.

(D-E) Staining and quantification of CC1 and MBP in the hippocampus. Scale bar: 50 μm. n = 4 mice

(F-G) Electron microscopy image of corpus callosum sections and quantification of myelinated axon number and g-ratio. Scale bar, 10 μm. n = 3 mice.

(H-I) PDGFRα staining and quantification of $PDGFR\alpha^+$ area of each OPC and the number of OPC in the hippocampal CA1 region. Scale bar, 50 μm. n = 4 mice.

(J-K) Representative images of NG2^{CreERT}:tdTomato, and quantification of the process coverage per cell. Scale bar, 20 μm. n = 4 mice.

Plots show individual data and mean ± SD; n.s., not significant, *p < 0.05, **p < 0.01, ****p < 0.0001; two-sided Student's t-test.

See also Figure S2 and S3.

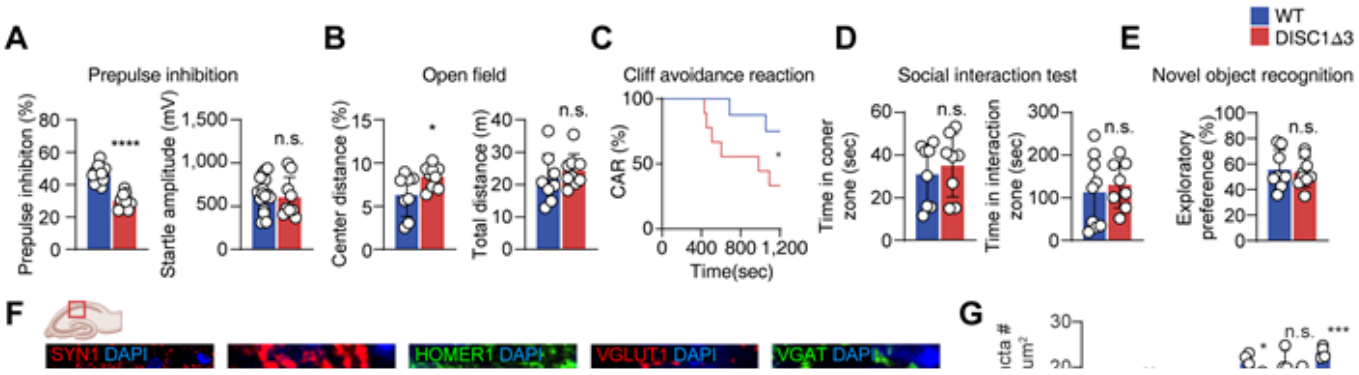

Figure 3

Oligodendroglial DISC1-Δ3 variant triggers schizophrenia-like behaviors and synaptic defects

(A-E) Behavioral tests on WT and DISC1-Δ3 mice, including prepulse inhibition test (A), open field test (B), cliff avoidance reaction (CAR) test (C), social interaction test (D), and novel object recognition (E). n = 8, 9 mice from each group.

(F) Staining of synaptic elements, including SYN1 (presynaptic marker), HOMER1 (postsynaptic marker), VGLUT1 (glutamatergic synaptic marker), and VGAT (GABAergic synaptic marker) in the hippocampal CA1 region. Scale bar is 5 μm.

(G) Quantification of SYN1 in different hippocampal and cortical regions. n = 4 mice of each genotype (DG, dentate gyrus. RSG, granular retrosplenial area. RSA, agranular retrosplenial area. V2MM, secondary visual cortex, mediomedial area).

(H) Quantification of different synaptic elements in the CA1 region. n = 4 mice of each genotype.

(I) Representative traces of sEPSCs and sIPSCs recordings from P23 hippocampal slices.

(J) Quantification of the frequency and amplitude of sEPSCs. n = 15, 18 cells from 3 mice of each genotype.

(K) Quantification of the frequency and amplitude of sIPSCs. n = 15, 18 cells from 3 mice of each genotype

Plots show individual data and mean ± SD; n.s., not significant, *p < 0.05, **p < 0.01, ***p < 0.001; two-sided Student's t-test, or log-rank test for survival curve.

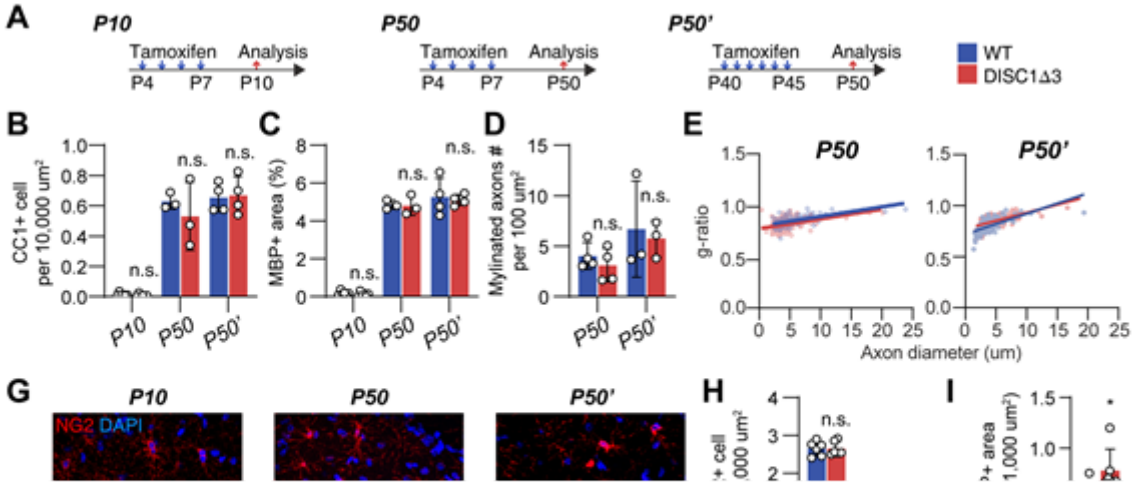

Figure 4

Induction of DISC-Δ3 results in **OPCs hypertrophy but does not affect myelination.**

(A) 3 different experiment setups of oligodendroglial DISC-Δ3 induction.

(B) Quantification of CC1 numbers in the hippocampus in three different setups. n = 6, 3, or 4 mice.

(C) Quantification of MBP^{+} area in the hippocampus in three different setups. n = 6, 3, or 4 mice.

(D) Quantification of myelinated axon numbers in the second and the third setups. n = 3 or 4 mice.

(E-F) g-ratio chart in the second and the third setups.

(G) Immunostaining of NG2 in three different experiment setups. Scale bar, 10 μm.

(H) Quantification of $NG2^+$ OPC number and $NG2^+$ area per OPC in (G). n = 6, 3, or 4 mice.

(I) Quantification of GFP^+ or $tdTomato^+$ area per cell in P10 $NG2^{CreERT}$:mT/mG or $NG2^{CreERT}$:tdTomato mice. n = 6 mice.

(J) Staining of NeuN in $NG2^{CreERT}$:mT/mG brain section. Arrowheads highlight the neuron cell bodies enwrapped by membrane GFP (mGFP)-labeled OPC. Scale bar, 100 μm or 10 μm.

(K) 3D reconstruction of high magnification images in (J). Scale bar, 10 μm.

(L) 3D reconstruction of SYN1 staining in the CA1 region of a $NG2^{CreERT}$:mT/mG brain section. Asterisks: the adjacent neuronal nucleus. Scale bar, 5 μm.

(M) Quantification of the percentage of neuronal cell body enwrapped by $mGFP^+$ OPC processes. N = 3 mice.

(N) Quantification of the number of neurons with cell body contacted by $mGFP^+$ OPC. n = 3 mice.

Plots show individual data and mean ± SD; n.s., not significant, *p < 0.05, **p < 0.01, ***p < 0.001; two-sided Student's t-test.

See also Figure S4.

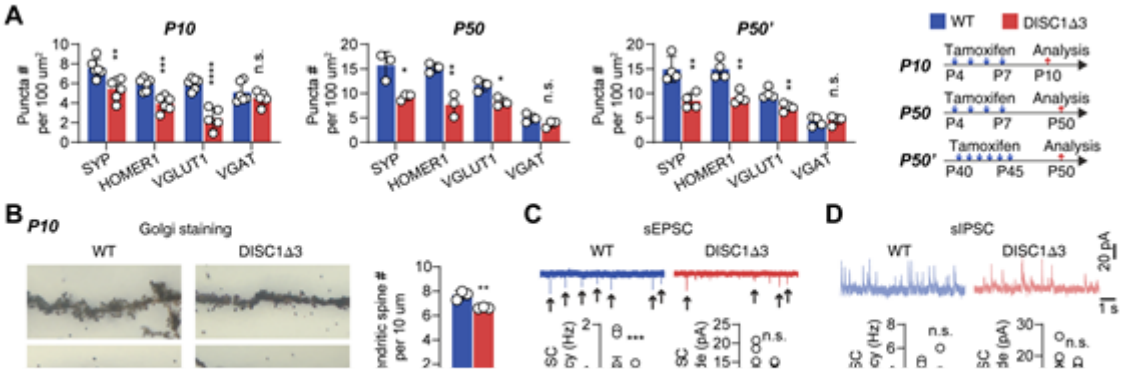

Figure 5

Aberrant OPC but not myeination deficits contribute to the onset of schizophrenia-like symptoms in DISC1-Δ3 mice

(A) Quantification of synaptic elements in CA1 region of three different experiment setups. n = 3~6 mice.

(B) Golgi staining and quantification of the dendritic spines of hippocampal neurons. Scale bar, 5 μm. n = 3 mice.

(C-D) Representative traces of sEPSCs and sIPSCs recording from P10 hippocampal slices and statistics of sEPSCs and sIPSCs. n=19, 20 cells from 3 mice of each genotype.

(E-F) Behavioral test of mice from the second and the third experiment setups. n > 7 mice.

(G) PLP^{CreERT} mice was mated to $DISC1^{exon3\ f/+}$ mice to produce PLP^{CreERT}: $DISC1^{exon3\ f/+}$ (OL DISC1-Δ3) mice. Mice were treated with tamoxifen from P4 to P7, and sacrificed at P23 for analysis.

(H) Staining and quantification of SYN1 in the hippocampus CA1 region in OL DISC1-Δ3 mice. n = 3 mice.

(I) Staining and quantification of MBP in OL DISC1-Δ3 mouse hippocampus. n = 3 mice.

(J) Staining of PDGFRα and quantification of $PDGFR\alpha^+$ area per cell in OL DISC1-Δ3 mouse hippocampus. n = 3 mice.

(K) Staining of NG2 in primary OPC culture and quantification of $NG2^+$ area per OPC. Scale bar, 5 μm. n = 9 experiments.

(L) Staining of MAP2 and SYN1 in primary OPC-neuron co-culture and quantification of $SYN1^+$ puncta on dendrite. Scale bar, 10 μm. n = 6 experiments.

(M) Staining of MAP2 and SYN1 in primary neuron culture treated by OPC-conditioned medium (OPC-CM) and quantification of $SYN1^+$ puncta on dendrite. Scale bar, 10 μm. n = 6 experiments.

Plots show individual data and mean ± SD; n.s., not significant, *p < 0.05, **p < 0.01, ***p < 0.001, ****p < 0.0001; two-sided Student's t-test.

See also Figure S5.

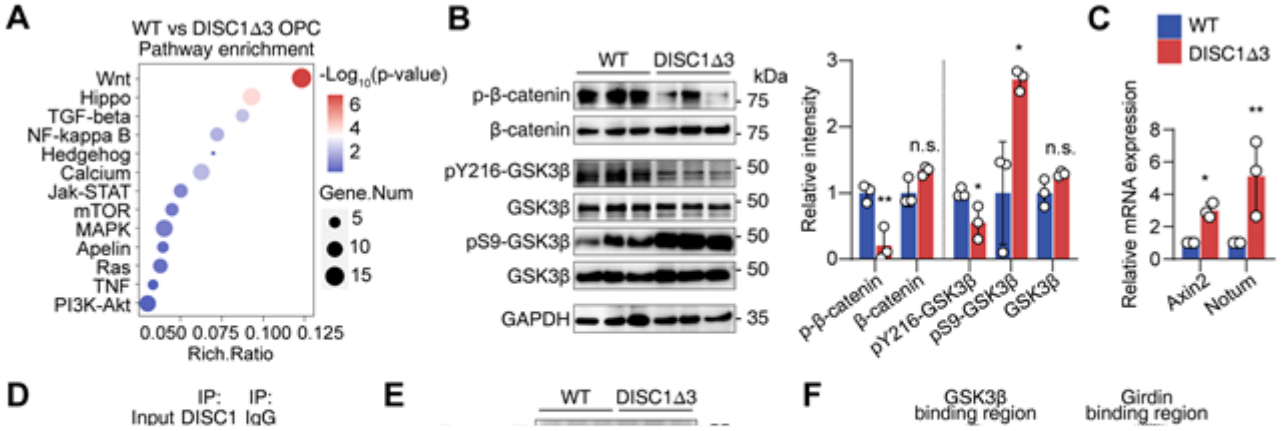

Figure 6

Aberrant Wnt/β-catenin activation in DISC1-Δ3 OPCs.

(A) KEGG pathway analysis of differentially expressed genes revealed by RNA-seq between acutely isolated WT and DISC1-Δ3 OPCs.

(B) Western blot and quantification of β-catenin and GSK3β phosphorylation in isolated WT and DISC1-Δ3 OPCs. n = 3 mice.

(C) RT-qPCR of canonical Wnt pathway targets Axin2 and Notum in isolated OPCs. n = 3 mice.

(D) Co-immunoprecipitation experiments in primary WT or DISC1-Δ3 OPCs using anti-DISC1 or normal IgG antibodies, followed by immunoblotting with Girdin and GSK3β antibody. Lower panel is the quantification of Girdin and GSK3β band intensity in DISC1 pull down normalized to Input. n = 3 experiments.

(E) Western blot and quantification of AKT phosphorylation in isolated WT and DISC1-Δ3 OPCs. n = 3 mice.

(F) Model of DISC1-Δ3 regulation on Wnt/β-catenin signaling pathway. DISC1-Δ3 protein retains the GSK3β binding region but not the Girdin binding region. Both full length DISC1 and DISC1-Δ3 bind with GSK3β, directly inhibiting its activity, whereas DISC1-Δ3 could not bind to Girdin to inhibit AKT activity, leading to further suppression of GSK3β activity and subsequent hyperactivated Wnt/β-catenin signaling.

(G) Representative images of RNF43 staining in each control and schizophrenia patient hippocampal sections. Arrowheads highlight $RNF43^{+}$ cells. Scale bar, 50 μm.

(H) Quantification of RNF43 intensity in (G). n = 5 age-matched samples.

Plots show individual data and mean ± SD; n.s., not significant, *p < 0.05, **p < 0.01, ***p < 0.001; two-sided Student's t-test (paired t-test for age-match human samples).

See also Figure S6.

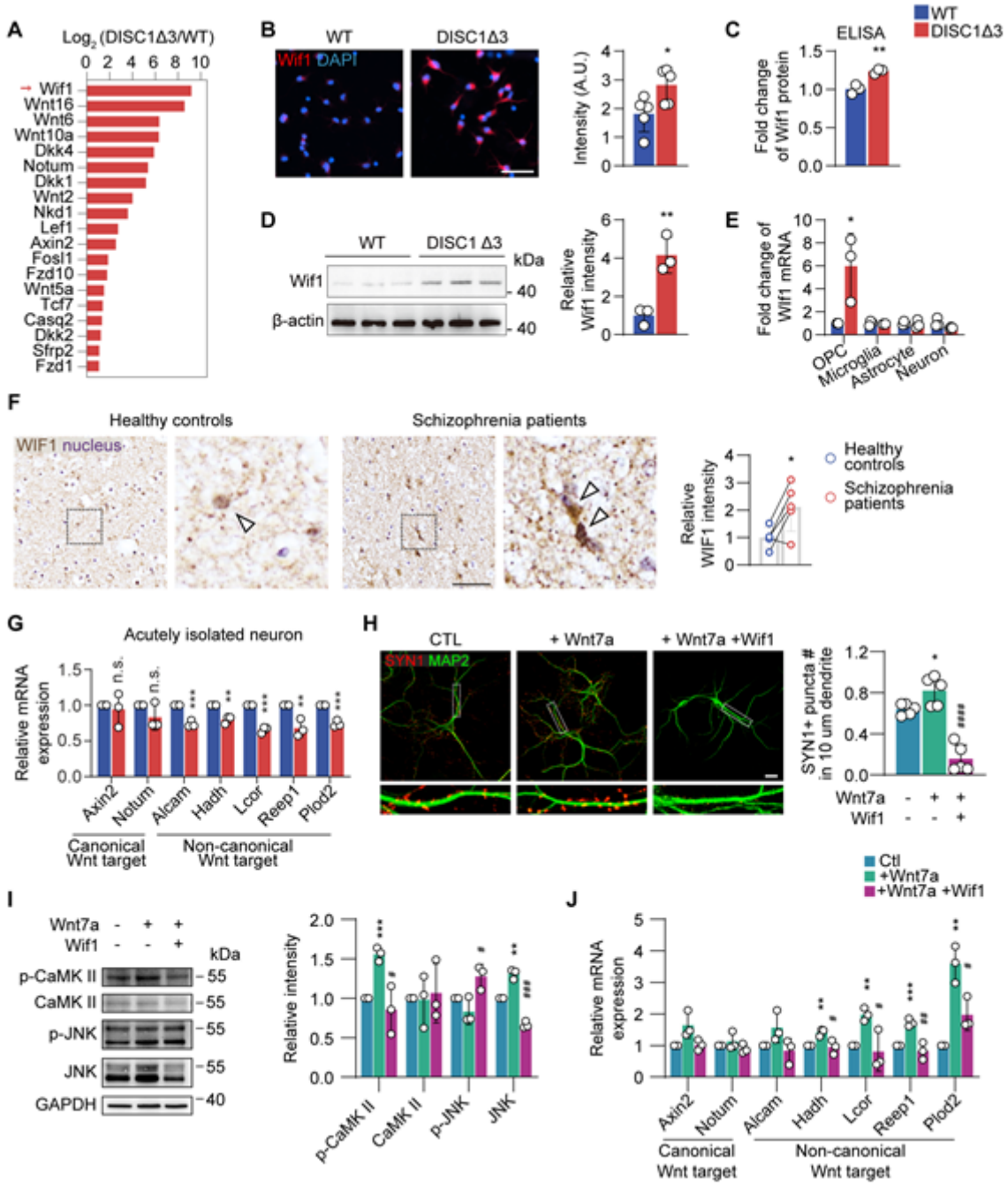

Figure 7

Upregulated Wif1 in DISC1-Δ3 OPCs suppresses synaptogenesis by a non-canonical Wnt pathway.

(A) Wnt pathway-related genes are upregulated in DISCΔ3 OPCs shown by RNA-seq. Arrow highlights Wif1.

(B) Staining and quantification of Wif1 in cultured OPCs. Scale bar, 50 μm. n = 5 experiments.

(C) ELISA of Wif1 in WT or DISC-Δ3 mouse brain lysates. n = 3 mice.

(D) Western blot and quantification of Wif1 expression in OPCs. n = 3 mice.

(E) RT-qPCR of Wif1 expression in acutely isolated OPC, microglia, astrocytes, and neurons from WT or DISC-Δ3 mice. n = 3 mice.

(F) Immunohistochemistry and quantification of Wif1 in hippocampal slice of controls and schizophrenia patients. Arrowheads highlight $WIF1^+$ cells. n = 5 samples per group.

(G) RT-qPCR experiment of acutely isolated neurons from WT and DISC1-Δ3 mice to detect expression of canonical and non-canonical Wnt pathway target gene expression. n = 3 mice.

(H) Staining of SYN1 and MAP2 in primary hippocampal neurons cultured with or without Wnt7a or Wif1. Right: quantification of SYN1 puncta on dendrites. CTL, control. Scale bar, 10 μm. n = 5 experiments.

(I) Western blot and quantification of CaMK II and JNK phosphorylation in protein lysates from primary hippocampal neurons cultured with or without Wnt7a or Wif1. n = 3 experiments.

(J) RT-qPCR on primary hippocampal neuronal culture to detect expression of canonical and non-canonical Wnt pathway target gene expression. n = 3 experiments.

Plots show individual data and mean ± SD; *p < 0.05, **p < 0.01, ***p < 0.001; #, statistical analysis between Wnt7a treatment and Wnt7a+Wif1 treatment. #p < 0.05, ##p < 0.01, ###p < 0.001; two-sided Student's t-test.

See also Figure S7.

Figure 8

Suppressing expression of oligodendroglial Wif1 rescues synaptic loss and behavioral disorders in DISC1-Δ3 mice.

(A) Staining of synaptic elements in the hippocampus of P12 DISC1-Δ3 mice with Wif1-shRNA encoded retrovirus injection. Scramble shRNA encoded retrovirus serves as control. Scale bar, 5 μm.

(B) Quantification of synaptic elements in (A). n = 3 mice from each genotype.

(C) Staining of synaptic elements in the hippocampus of P10 Wif1 conditional KO DISC1-Δ3 Wif1 conditional KO mice. Scale bar, 5 μm.

(D) Quantification of synaptic elements in (C). n = 6 mice from each genotype.

(E) Representative results of sEPSC or sIPSC recording in P10 Wif1 conditional KO DISC1-Δ3 mice.

(F) Quantification of sEPSC frequency and amplitude. n = 18, 19 cells from 3 mice of each genotype.

(G) Quantification of sIPSC frequency and amplitude. n = 18, 19 cells from 3 mice of each genotype.

(H) Prepulse inhibition test of P23 Wif1 KO DISC1-Δ3 mice. n = 9, 10 mice of each genotype.

(I) Open field test of P23 Wif1 conditional KO DISC1-Δ3 mice. n = 9, 10 mice of each genotype.

Plots show individual data and mean ± SD; n.s., not significant, *p < 0.05, **p < 0.01, ***p < 0.001; two-sided Student's t-test.

See also Figure S8.

Supplementary Files

This is a list of supplementary files associated with this preprint. Click to download.

- DISC1OPCExtendeddataNatureMedicine.doc